Distant-neighbor exchange constants from magnetization steps in $Zn_{1-x}Co_xTe$

T. Q. Vu, V. Bindilatti,* and Y. Shapira
Department of Physics and Astronomy, Tufts University, Medford, Massachusetts 02155

E. J. McNiff, Jr. and C. C. Agosta
Francis Bitter National Magnet Laboratory, Massachusetts Institute of Technology, Cambridge, Massachusetts 02139

J. Papp, R. Kershaw, K. Dwight, and A. Wold
Department of Chemistry, Brown University, Providence, Rhode Island 02912

(Received 30 April 1992)

Direct measurements of several exchange constants J_i, for several neighbors located at different distances r_i, are possible via the magnetization-steps method. Predictions for the distance dependence of the exchange constant can then be tested. The theory of the magnetization steps (MS's) caused by distant neighbors is presented. This theory is based on a sequence of cluster models. The problem of identifying the particular exchange constant J_i that is responsible for an observed series of MS's is also discussed. The magnetization of $Zn_{1-x}Co_xTe$, with $x=0.007$, was measured at 0.6 K in magnetic fields up to 27 T, and at 0.08 K in fields up to 20 T. Two series of MS's were observed. These series were identified as being due to pairs of next-nearest neighbors (J_2 pairs), and pairs of third neighbors (J_3 pairs). The exchange constants deduced from the data are $J_2/k_B=-(5.7\pm0.6)$ K and $J_3/k_B=-(2.7\pm0.3)$ K. These values, and the earlier result $J_1/k_B=-38$ K for the nearest-neighbor exchange constant, are compared with several proposed dependences of J_i on distance.

I. INTRODUCTION

Exchange interactions between magnetic ions in dilute magnetic semiconductors (DMS's) have been the focus of many recent works. The present theoretical understanding of these interactions is largely based on the works of Larson, Hass, Ehrenreich, and Carlsson.[1-3] They showed that superexchange is the dominant exchange mechanism, and that in II-VI DMS's the nearest-neighbor (NN) exchange constant J_1 is the largest constant by far. The main techniques for measuring J_1 are the susceptibility method,[4] inelastic neutron scattering,[5] and magnetization steps.[6] These techniques have been reviewed recently.[7] In the Mn-based II-VI DMS's, a typical value of J_1 is $J_1/k_B\sim-10$ K. For Co-based II-VI DMS's, J_1 is typically higher, $J_1/k_B\sim-40$ K. For $Zn_{1-x}Co_xTe$, which is the material studied in the present work, $J_1/k_B=-38$ K.[5]

In a given DMS there are many exchange constants: J_1 for NN's, J_2 for next-nearest neighbors (2nd neighbors), J_3 for 3rd neighbors, etc. Qualitatively, the exchange constants J_i are expected to decrease with the distance r_i of the ith neighbor. However, the precise manner in which J_i decreases with r_i is not well established.[8] The dependence of J_i on r_i may be expressed as a continuous function $J=J(r)$, which is to be evaluated only at the discrete set of distances $r=r_i$. Examples of problems that require knowledge of $J(r)$ are the dependence of the spin-glass transition temperature on the concentration x of magnetic ions,[9] and calculations of the specific heat,[9,10] and of the magnetization.[9]

Various predictions, or suggestions, for the dependence of J on r have been made. In the theory of Larson *et al.*[1] the r dependence for J_1 through J_4 is approximately

$$J\propto\exp[-4.89(r/a)^2]\ , \tag{1}$$

where a is the lattice constant. This result is independent of the cation or anion in the parent (nonmagnetic) semiconductor. However, because Eq. (1) was obtained specifically for exchange interactions between Mn^{2+} ions, it may not apply to the Co^{2+} ions studied in the present work. For the zinc-blende structure Eq. (1) gives

$$J_2/J_1=J_3/J_2=J_4/J_3\cong0.1\ .$$

A much weaker r dependence for the exchange constants J_2 through J_4 was suggested by Bruno and Lascaray.[11] According to them,

$$J_2=2J_3=4J_4\ . \tag{2}$$

This suggestion is based on the notion that the exchange paths for distant neighbors consist of consecutive links, each being the same as the link for nearest neighbors (which is through the intervening anion). For a given distant neighbor there may be several alternative exchange paths, which are all equivalent. The exchange paths responsible for J_2, J_3, and J_4 are all similar, but the number of equivalent exchange paths is different for each of these three J_i's. The ratios 1:2:4 in Eq. (2) are simply the ratios of the numbers of equivalent exchange paths for the three J_i's. The ratio J_2/J_1 was not predicted by Bruno and Lascaray.

An algebraic dependence of J on r has been proposed in some papers,[8-10] namely, $J\propto r^{-n}$. This proposal was

put forward on empirical grounds, i.e., it gave good fits to several sets of data. The reported values for n in II-VI DMS's are between 5 and 8 (Ref. 8). The ratio J_3/J_2 calculated from this algebraic dependence is then between 0.20 and 0.36, which is intermediate between the values predicted by Larson *et al.* and by Bruno and Lascaray. The ratio $J_2/J_1 \sim 0.1$ is similar to that of Larson *et al.*

Early determinations of distant-neighbor exchange constants (i.e., J_i other than the NN exchange constant J_1) were based on indirect methods. They involved fits in which J_2, or both J_2 and J_3, were treated as adjustable parameters.[12] Recently, however, direct measurements of distant-neighbor exchange constants became possible, using the magnetization steps (MS's).[13] In the present work this method was employed to determine both J_2 and J_3 in $Zn_{1-x}Co_xTe$.

II. THEORY

Previous works on the MS's were largely devoted to MS's that arise from pairs of *nearest-neighbor* magnetic ions.[6,7] In what follows, we focus primarily on the theory for MS's that arise from pairs of *distant neighbors*. One problem that is addressed is how to identify the particular J_i that gives rise to an observed series of MS's.

A. Isolated pairs of spins

We start with a brief summary of some basic results that will be needed later. Consider an isolated pair of identical spins, $\mathbf{S}_1$ and $\mathbf{S}_2$, coupled to each other by an antiferromagnetic exchange interaction

$$\mathcal{H}_{\text{exch}} = -2J\mathbf{S}_1\cdot\mathbf{S}_2 \ . \tag{3}$$

Here, J can be any one of the J_i's, which are all assumed to be antiferromagnetic. In zero magnetic field, $H=0$, the energy levels of such a pair depend only on the magnitude S_T of the total spin of the pair, i.e.,

$$E = -J[S_T(S_T+1)-2S(S+1)] \ , \tag{4}$$

where $S=S_1=S_2$ is the magnitude of the individual spins. The value of S_T in the ground state is zero, corresponding to an antiparallel alignment of the two spins. The excited states are higher by $2|J|$, $6|J|$, $12|J|$, ..., corresponding to $S_T=1,2,3,\ldots,2S$. For Co^{2+} ions in the zinc-blende structure the value of S is 3/2 (Refs. 14,15). Figure 1(a) shows the zero-field energies for a pair of such Co^{2+} ions.

When a uniform magnetic field **H** is applied, the energy levels undergo a Zeeman splitting, as shown in Fig. 1(b). The energy levels are now governed by both S_T and the component m of $\mathbf{S}_T$ along **H**. The crucial point in Fig. 1(b) is that the ground state changes at the fields H_1 H_2, and H_3. Each change increases the value of $|m|$ for the ground state by one unit. These jumps of $|m|$ correspond to jumps in the component of the magnetic moment of the ground state along **H**.

Consider now an ensemble of identical pairs. At low temperatures, $k_BT \ll 2|J|$, the magnetization of such a system will exhibit a series of MS's at the fields H_n. These MS's are shown in Fig. 1(c). The fields H_n at the centers of the MS's are given by

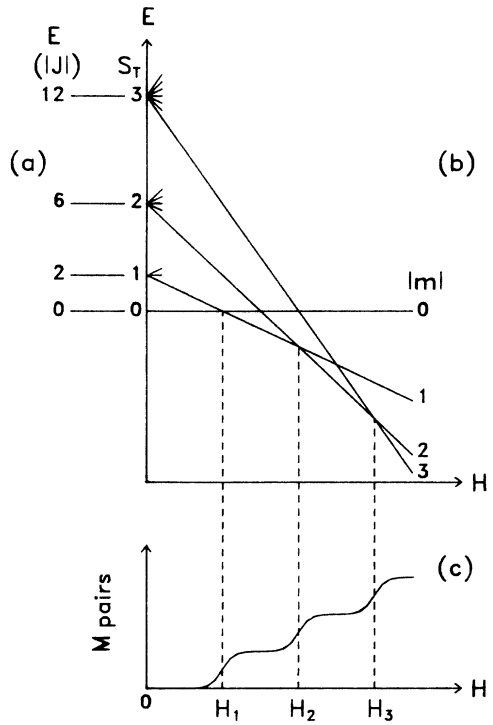

FIG. 1. (a) Energy level diagram for an isolated pair of Co^{2+} ions at $H=0$. E is the energy in units of $|J|$, where J is the exchange constant. S_T is the magnitude of the total spin of the pair. (b) Zeeman splitting of these energy levels in a magnetic field H. Note the level crossings at H_n, which change the ground state. (c) The magnetization M_{pairs} of an ensemble of identical pairs at low temperatures.

$$g\mu_B H_n = 2|J|n \ , \tag{5}$$

where $n=1,2,3$ for Co^{2+} pairs. Equation (5) applies only to the idealized case of isolated pairs. It will be modified slightly later.

B. Cluster models

In this section a sequence of cluster models is considered. It is assumed that all exchange interactions are antiferromagnetic ($J_i<0$), and that the magnitude of $J_i(r_i)$ decreases with the distance r_i.

I. The J_1 model

In the J_1 model (or nearest-neighbor cluster model[16]), only the largest exchange constant, J_1, is included. All other exchange constants are set equal to zero. The spins in the sample are then viewed as belonging to clusters of various sizes. The smallest cluster is a "single," with no magnetic nearest neighbors to which it can couple. The next cluster in size is a J_1 pair, consisting of two spins coupled by J_1. Next in size are two types of J_1 triplets (open and closed), followed by various types of J_1 quartets, J_1 quintets, etc.

For the samples used in the present work the cobalt

concentration is $x=0.007$. Assuming a random distribution of the cobalt ions over the cation sites, 91.9% of the spins are then singles, 7.4% are in J_1 pairs, and only 0.7% are in larger clusters.[17] The magnetization for such a low value of x is therefore well approximated by the sum of the magnetizations of the singles and of the J_1 pairs.

A schematic of the magnetization curve at temperatures $k_BT \ll 2|J_1|$ is shown in Fig. 2(a). The initial rise of the magnetization M is due to the singles, which align readily parallel to **H**. The three magnetization steps at higher fields (marked by arrows) are due to the J_1 pairs. We shall refer to these MS's as "J_1 steps." In the J_1 model the magnetic fields at the centers of the J_1 steps are still given by Eq. (5), with $J=J_1$.

Magnetization steps may also arise from J_1 clusters larger than J_1 pairs, e.g., J_1 triplets.[13,16] However, for the low value of x in the present samples the MS's due to these larger J_1 clusters should be too small to be of any significance.

2. J_1-J_2 model

In the J_1-J_2 model the largest two exchange constants, J_1 and J_2, are both included. All other J_i's are set equal to zero.

There are four categories of clusters in this model: (1) singles, with no magnetic NN's or next-nearest neighbors (NNN's), (2) pure J_1 clusters, in which the spins are connected only by J_1 "bonds," (3) pure J_2 clusters, and (4) mixed J_1-J_2 clusters, with both J_1 and J_2 bonds. Each of the last three categories of clusters contains clusters of different types. For example, among the pure J_1 clusters are pure J_1 pairs and pure J_1 open triplets. Similarly, there are pure J_2 pairs, pure J_2 open triplets, and still other types of pure J_2 clusters. The simplest mixed J_1-J_2 cluster is the J_1-J_2 open triplet, consisting of a chain of three spins connected by a single J_1 bond and a single J_2 bond. The probabilities of finding various types of clusters in the J_1-J_2 model were first given by Kreitman and Barnett.[18]

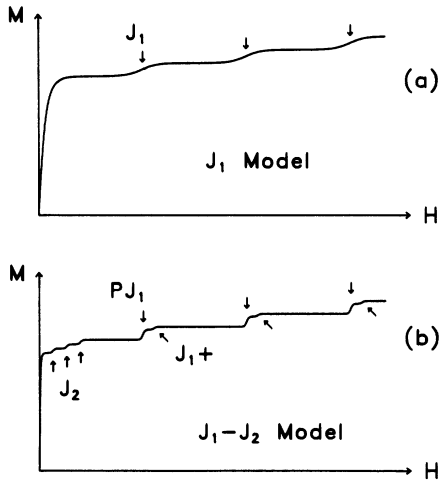

FIG. 2. (a) The magnetization curve, M vs H, in the J_1 model. Note the three J_1 steps. These results are for $k_BT \ll 2|J_1|$. (b) The magnetization curve in the J_1-J_2 model. Note the three J_2 steps, and the fine structure in the J_1 steps. The fine structure is due to pure J_1 pairs (PJ_1) and J_1-J_2 open triplets (J_1+). The results in part (b) are for $k_BT \ll 2|J_2|$.

The inclusion of J_2 in the J_1-J_2 model leads to new features in the magnetization curve, i.e., features that were not present in the J_1 model. The most important new feature is an additional series of MS's, which arise from the J_2 pairs. These "J_2 steps" are indicated in Fig. 2(b) by the upward-pointing arrows. The magnetic fields at the J_2 steps are given by Eq. (5) with $J=J_2$. These fields are much lower than those at the J_1 steps. To observe the J_2 steps, k_BT must be small compared to $2|J_2|$. Even for Co^{2+} ions, which have relatively strong exchange interactions, this temperature requirement is met only below 1 K. It is largely because of this temperature requirement that the J_2 steps were observed only recently.[13]

The inclusion of J_2 also leads to a fine structure in the J_1 steps. The J_1 steps in Fig. 2(a) are due to J_1 pairs in the J_1 model. Once J_2 also is included, only a fraction of these "original" J_1 pairs will remain pure J_1 pairs. The other original J_1 pairs will be coupled to other spins by J_2 bonds, so that they will find themselves in mixed J_1-J_2 clusters. Those original J_1 pairs that remain pure J_1 pairs in the J_1-J_2 model will give rise to MS's at exactly the same fields as in the J_1 model [i.e., Eq. (5) with $J=J_1$]. In Fig. 2(b) these "pure" J_1 MS's are indicated by the downward-pointing arrows marked as PJ_1. The other original J_1 pairs, which find themselves in mixed J_1-J_2 clusters, will give rise to MS's at higher fields. For low x, the J_1-J_2 open triplet is the most probable mixed J_1-J_2 cluster. The MS's due to the J_1-J_2 open triplets are indicated in Fig. 2(b) by the slanted arrows, marked as J_1+. Other mixed J_1-J_2 clusters will give rise to still other MS's, but these should be smaller in size than the J_1+ MS's if x is low. For the concentration $x=0.007$ in the present samples, 94.5% of the original J_1 pairs remain pure J_1 pairs, 4.9% find themselves in J_1-J_2 open triplets, and only 0.6% are in other mixed J_1-J_2 clusters.

In our terminology the name J_1 steps refers to all MS's that involve the original J_1 pairs in the J_1 model. The PJ_1 and J_1+MS's (in the J_1-J_2 model) are special types of J_1 steps. At temperatures $k_BT \ll |J_2|$, both the PJ_1 and J_1+ MS's may be resolved, as in Fig. 2(b). Each of the original J_1 steps in Fig. 2(a) has then developed a fine structure consisting of a PJ_1 step and the adjacent J_1+ step. Additional fine structure may appear due to other types of J_1-J_2 clusters in which the original J_1 pairs find themselves.

The J_1+ MS's are due to J_1-J_2 open triplets. The fields at which they occur may be expressed as

$$g\mu_B H_n = 2|J_1|n + \epsilon_n \ . \tag{6}$$

The correction ϵ_n, which does not appear in Eq. (5), is positive and is due to the antiferromagnetic J_2 bond in

the open triplet. This correction was calculated by solving the triplet problem numerically. The results for $S=3/2$ (appropriate for Co^{2+} ions) are shown in Fig. 3. Clearly, ϵ_n is of order $|J_2|$, but the ratio $\epsilon_n/|J_2|$ depends both on J_2/J_1 and on n. In the limit $J_2/J_1 \ll 1$, the ratio $\epsilon_n/|J_2|$ is independent of n and is equal to 1.5. This result agrees with that obtained earlier[7] for $S=3/2$ on the basis of the effective-field method of Larson *et al.*[12] Okada's approximate solution of the triplet problem in the small J_2 limit[19] also leads to the same result.[7] Note, however, that for $J_2/J_1 \sim 0.1$, which is a realistic value, the ratio $\epsilon_n/|J_2|$ in Fig. 3 depends somewhat on n, and is greater than 1.5. For $J_1=J_2$, Fig. 3 gives $\epsilon_n=3|J_2|$, independent of n. This result agrees with that obtained earlier for J_1 open triplets, which are equivalent to J_1-J_2 open triplets when $J_2=J_1$.

Often the fine structure in the J_1 steps is not resolved because the temperature is too high, or because the Dzyaloshinki-Moriya interaction produces an additional broadening.[20] In that case, J_2 (and also the other distant-neighbor exchange constants, J_3, J_4, etc.) influence the J_1 steps in two ways. First, the unresolved fine structure due to the distant neighbors produces an additional broadening. Second, the centers of the J_1 steps are at somewhat higher fields than those given by Eq. (5), i.e.,

$$g\mu_B H_n = 2|J_1|n + \Delta_n \ , \tag{7}$$

where $\Delta_n > 0$. In the effective-field treatment of Larson *et al.*[12] the shift Δ_n is independent of n. In that case the field separation between adjacent J_1 steps is independent of n and is given by

$$g\mu_B(H_{n+1}-H_n)=2|J_1| \ . \tag{8}$$

The determination of J_1 from the fields at the J_1 steps is usually based on Eq. (8). As pointed out earlier, in connection with the correction ϵ_n in Eq. (6), the effective-field method may be somewhat inaccurate for realistic values of J_2/J_1. Nevertheless, we expect that the error in J_1 resulting from the use of Eq. (8) will be typically less than 2%.

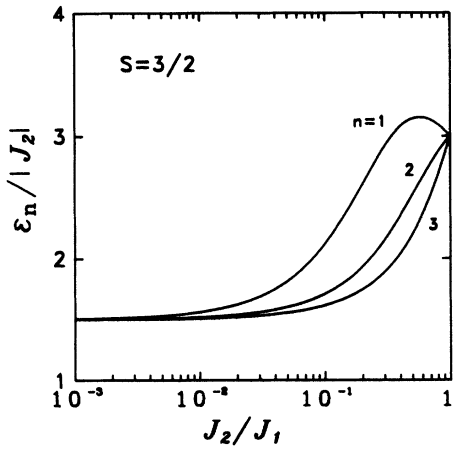

FIG. 3. The shift ϵ_n in Eq. (6) as a function of J_2/J_1. The curves are for the three J_1 steps ($n=1,2,3$).

3. J_1-J_2-J_3 model and other cluster models

In the J_1-J_2-J_3 model, the largest three exchange constants are included, but no others. The various clusters (up to triplets) which appear in this model, and their probabilities, were given by Pohl and Busse.[21] Among the new clusters that did not exist in the J_1-J_2 model are the J_3 pairs. These J_3 pairs lead to a new series of MS's, i.e., J_3 steps.

The inclusion of J_3 also leads to a fine structure in the J_2 steps, and to an additional fine structure in the J_1 steps. We focus on the fine structure in the J_2 steps. By definition, J_2 steps consist of all MS's that arise from the original J_2 pairs in the J_1-J_2 model. In that model, all J_2 pairs are pure so that there is only one type of J_2 steps. However, when J_3 too is included the J_2 steps develop a fine structure, corresponding to several types of J_2 steps. One type (PJ_2) are MS's arising from pure J_2 pairs in the J_1-J_2-J_3 model. Another type (J_2+) are MS's arising from J_2-J_3 open triplets, and there are still other types. [For the concentration $x=0.007$ in the present samples, 80% of the original J_2 pairs (in the J_1-J_2 model) remain pure J_2 pairs when J_3 too is included.] If the fine structure caused by J_3 is not resolved then the fields at the J_2 steps are given by Eq. (7) with J_1 replaced by J_2. The exchange constant J_2 is then obtained from the difference $(H_{n+1}-H_n)$ by using Eq. (8) with J_1 replaced by J_2. The same equation can also be used to determine J_2 when exchange constants beyond J_3 (e.g., J_4) produce additional unresolved fine structure in the J_2 steps.

The next cluster model in the sequence is the J_1-J_2-J_3-J_4 model. The inclusion of J_4 in the model leads to J_4 steps, to a fine structure in the J_3 steps, and also to additional fine structure in the J_2 steps and in the J_1 steps. When the fine structure in the J_3 steps is not resolved, the exchange constant J_3 is obtained from the field separations between adjacent J_3 steps, i.e., Eq. (8) with J_1 replaced by J_3. The sequence of cluster models can be continued, leading to J_5 steps, etc.

C. Identifying the relevant exchange constant

Once a series of MS's has been observed, and the value of the exchange constant J responsible for it has been determined, it is still necessary to associate that J with a particular neighbor. That is, one has to decide if that J is J_1, or J_2, or J_3, or some other J_i. In most cases an approximate value for the dominant exchange constant J_1 is already known from the Curie-Weiss temperature. In such cases it is immediately obvious whether J is or is not J_1. If it is not, then the task of identifying the distant neighbor i becomes more difficult.

Suppose that all possible series of J_i steps, up to a certain value of i, have been observed. Since the magnitude of J_i is expected to decrease with increasing i, the series

at highest fields is due to J_1, the next series in order of decreasing H is due to J_2, etc., [cf. Fig. 2(b)]. Thus, in principle, the order in which the various series of MS's occur (starting at the highest fields and moving toward lower H) can be used to identify each series. In practice, however, this procedure is not always reliable. Even if J_1 is known, one may not be sure that the J_2 steps were not missed because the available magnetic field was not high enough to reach these steps. In addition, one may not be sure that the experimental resolution (for M) was adequate to observe all the series. For these reasons, two additional methods of identifying the relevant J_i have been suggested.[13] Here, we discuss only one of them, which proved to be helpful in the present work. The method focuses on the magnitude δM of the magnetization rise near each of the magnetization steps.

Consider a series of J_i steps arising from J_i pairs with a particularly index i. The size δM of each step in the series is determined by the number of J_i pairs. The latter number can be calculated by assuming that the magnetic ions are randomly distributed. (The strong evidence supporting this assumption is summarized in Ref. 6.) The number of J_i pairs is proportional to the probability P_{Ji} that a magnetic ion is a member of a J_i pair. The probabilities P_{Ji} for different i are known for the various cluster models.[17–19,21] If the steps are J_2 steps then their size will be governed by the probability P_{J2} in the J_1-J_2 model. This P_{J2} is shown as a solid line in Fig. 4(a). Here, a zinc-blende structure (appropriate for $Zn_{1-x}Co_xTe$) was assumed. The probabilities P_{J3} in the J_1-J_2-J_3 model, and P_{J4} in the J_1-J_2-J_3-J_4 model are shown in Figs. 4(b) and 4(c), respectively. These two probabilities govern the sizes of the J_3 and J_4 steps.

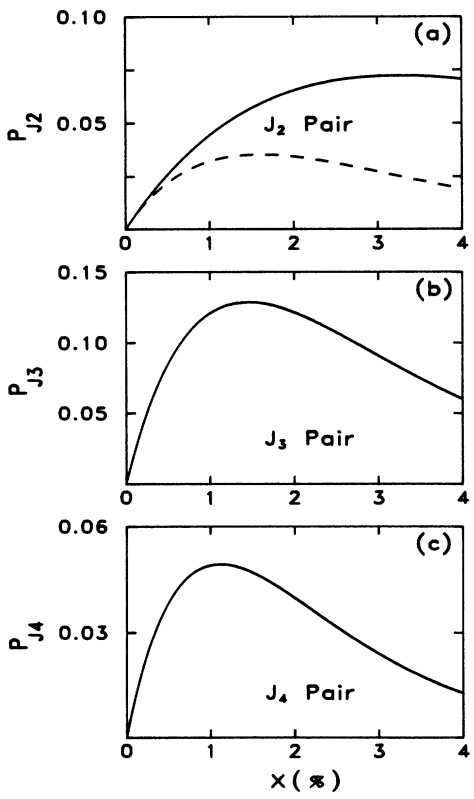

FIG. 4. (a) The probability P_{J2} that a magnetic ion is in a J_2 pair. The solid curve shows P_{J2} in the J_1-J_2 model, while the dahsed curve shows P_{J2} in the J_1-J_2-J_3 model. (b) The probability P_{J3} that a magnetic ion is in a J_3 pair, as given by the J_1-J_2-J_3 model. (c) The probability P_{J4} that a magnetic ion is in a J_4 pair, as given by the J_1-J_2-J_3-J_4 model. All the results are for the zinc-blende structure, in which the cations form an fcc lattice. A random distribution is assumed.

In order to associate a series of MS's with a particular J_i, the observed size of a step is compared with the various possible sizes calculated from the different probabilities P_{Ji}. For $x<1\%$, the J_3 steps are predicted to be much larger than the J_2 steps, essentially because there are 24 third neighbors compared to 6 second neighbors. This size difference is helpful in deciding if the series is due to J_2 pairs or to J_3 pairs.

One complication that occurred in the present work was that the ratio J_3/J_2 was about 0.5, i.e., not very small. In that case the observed J_2 steps should correspond to pure J_2 pairs in the J_1-J_2-J_3 model rather than to J_2 pairs in the J_1-J_2 model.[22] The size of a J_2 step is then governed by the probability P_{J2} in the J_1-J_2-J_3 model. This P_{J2} is shown as a dashed curve in Fig. 4(a). Fortunately, for the concentration $x=0.7\%$ in the present experiments the difference between P_{J2} in the J_1-J_2 model and P_{J2} in the J_1-J_2-J_3 model [solid and dashed curves in Fig. 4(a)] is not large. In the data analysis, P_{J2} of the J_1-J_2-J_3 model was actually used.

III. EXPERIMENTAL PROCEDURE

Two single crystals of $Zn_{1-x}Co_xTe$, referred to as sample A and sample B, were used. Both had been grown by chemical vapor transport under similar conditions, but at different times. Atomic absorption analysis gave $x=0.0068$ for sample A, and $x=0.0072$ for sample B. The values of x were also obtained by comparing the measured magnetization at the highest fields with the calculated "technical saturation value".[6,7,16] This gave $x=0.0072$ for sample A, and $x=0.0068$ for sample B. Compared to the atomic-absorption values the magnetization results for x in the two samples are in reverse order. These discrepancies, however, are compatible with the experimental accuracies of the two methods (about 3% for atomic absorption, and about 2% for the magnetization). In the data analysis we used $x=0.0070$ for both samples.

Two magnetometers were used to measure the magnetization M. The choice of magnetometer depended on the temperature. For measurements in liquid ^{3}He and liquid ^{4}He, from 0.6 to 4.2 K, a vibrating sample magnetometer (VSM) was used. The measurements with the VSM were performed both in a Bitter magnet with a maximum field of 20 T (200 kG) and in a hybrid magnet with a maximum field of 27 T. This VSM was designed to operate in the high-noise environment of these magnets. The signal from the VSM was proportional to M, but the proportionality constant (which depended some-

what on sample size and shape) was only known to within a few percent. Absolute calibration of M was achieved by comparing the VSM signal at 4.2 K and 5.0 T with the value measured with a Quantum-Design superconducting quantum interference device magnetometer.

Measurements in a dilution refrigerator, at $T \cong 0.08$ K, were performed in a 20 T Bitter magnet using a force magnetometer.[23] With this magnetometer, the signal from the sample was superimposed on a small monotonic background. Because the signal was small, due to the low value of x, the background was not negligible. The background did not obscure the MS's, but it prevented the determination of the size of the MS's in relation to the total magnetization. This problem did not exist with the VSM.

The size of each of the MS's was rather small, only 1–3 % of the total magnetization, which itself was small because of the low value of x. To improve the signal-to-noise ratio, several traces of M vs H were always taken under identical conditions. The traces were then averaged using a computer.

IV. RESULTS AND DISCUSSION

A. Two series of MS's

Two series of MS's, arising from two different distant neighbors, were observed. The analysis was complicated by the fact that the magnetic-field ranges in which the two series occurred overlapped to some extent. The two series were disentangled and identified only after the results of several experiments were compared to each other.

The overall behavior of the magnetization curves at low temperatures is illustrated by the data in Fig. 5. The solid curves show the measured magnetization of sample B at 4.2 and 0.6 K. The dashed curves are the same data, but after a correction for the diamagnetic susceptibility of the lattice, $\chi_d = -3.0 \times 10^{-7}$ emu/g (Ref. 24). At 4.2 K the MS's are not observed because of the large thermal broadening. At 0.6 K, on the other hand, three MS's are observed at the highest fields. These MS's stand out more clearly in the expanded plot shown in Fig. 6(a). Similar results were also obtained for sample A.

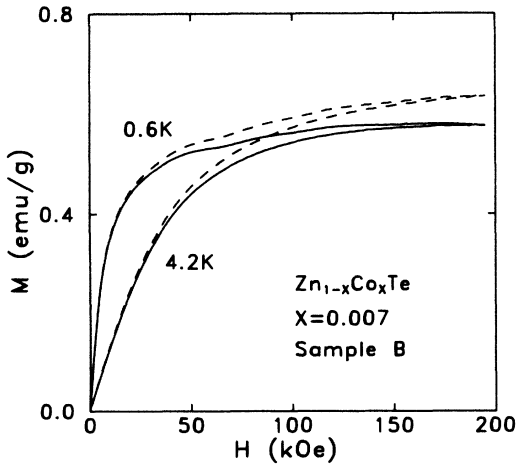

FIG. 5. Magnetization curves for sample B at 4.2 and 0.6 K. The solid curves show the measured magnetization. The dashed curves include a correction for the diamagnetic susceptibility of the lattice.

The derivative dM/dH of the data in Fig. 6(a) is shown in Fig. 6(b). The three MS's now appear as peaks. A single series of steps arising from Co^{2+} pairs should consist of three steps with equal separations between the steps. Although there are three MS's in Fig. 6(b), the separation between the third and second MS's appears to be somewhat larger than that between the second and first MS's. Thus, the three MS's may not belong to a single series.

Figure 7 shows the magnetization (plus some background) of sample B at 0.08 K. Similar data were also obtained for sample A. The derivative dM/dH for both samples at 0.08 K is shown in Figs. 8(a) and 8(b). For either sample there are now *four* prominent MS's, i.e., one more than expected for a single series. The three MS's at the highest fields correspond to the MS's in Fig. 6. It is now clear that these three MS's are indeed not equally spaced, so that they do not belong to a single series. On the other hand, the three MS's that are at the lowest fields seem to belong to the same series. One reason for this conclusion is that these three MS's are equally spaced. Another reason is that the ratios of the fields at which these MS's occur are approximately 1:2:3. Such field ratios are expected from the analog of Eq. (7) when the shift Δ is small compared to $2|J_i|$. The latter condition ($\Delta \ll 2|J_i|$) held in all previous experiments on MS's. Moreover, the unusually low value of x in the present experiments should have resulted in a low Δ, because the number of distant spins with which a pair in-

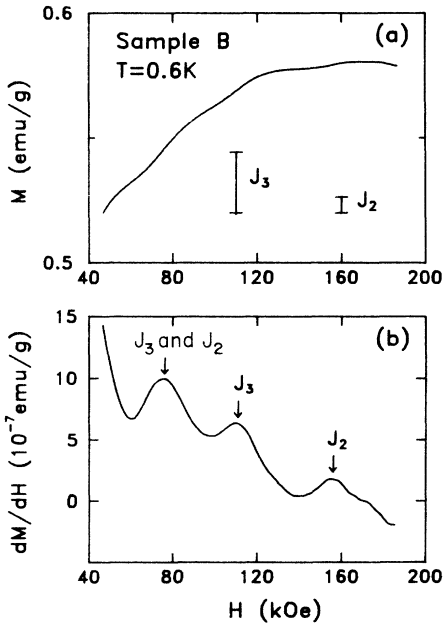

FIG. 6. (a) Upper portion of the 0.6 K data in Fig. 5. The bars are the calculated sizes for a J_2 step and for a J_3 step. (b) The derivative dM/dH obtained by a numerical differentiation of the data in part (a). The MS's are identified as J_2 steps, as J_3 steps, or as an overlap J_3andJ_2 of both types of steps.

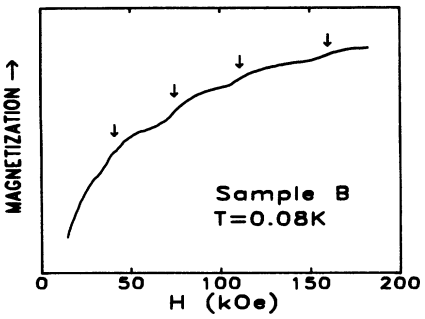

FIG. 7. The magnetization curve of sample B at 0.08 K. This curve contains a small monotonic background. The MS's are indicated by arrows.

teracts is smaller for a smaller x. The series consisting of the first three MS's (at the lowest fields) in Figs. 8(a) and 8(b) will be called the "first series."

The fourth MS in Figs. 8(a) and 8(b) (at $H \cong 160$ kOe) is the same as the highest-field MS in Fig. 6(b). This MS must belong to a "second series," which also consists of three steps. If the MS near 160 kOe were the highest-field member ($n=3$) of the second series then the lowest member should have occurred at roughly a third of this field, i.e., near 53 kOe. Since no MS is observed near this field [see Figs. 8(a) and 8(b)], it is likely that the MS near 160 kOe is either the first or the second member of the second series. If it is the first member ($n=1$) then the next member ($n=2$) should occur roughly at 320 kOe. If it is the second member ($n=2$) then the next member should occur roughly at 240 kOe.

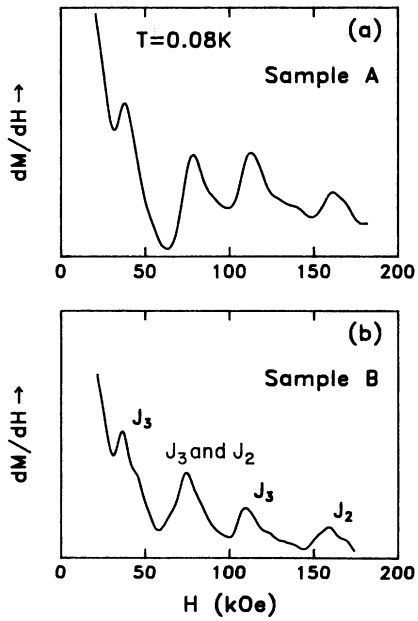

FIG. 8. The derivative dM/dH at 0.08 K. (a) Sample A. (b) Sample B. These curves were obtained by a numerical differentiation of the magnetization curves. The peaks are identified as J_2 steps, as J_3 steps, or as an overlap J_3 and J_2 of both types of steps.

To distinguish between these two possibilities, magnetization data up to 270 kOe were taken at 0.6 K using a hybrid magnet. The high-field portion of these data is represented by the solid curve in Fig. 9. There are two MS's in this field range, marked by arrows. Both MS's are comparable in size. The first MS, at 158 kOe, is also seen in Figs. 6, 7, and 8. The second MS in Fig. 9 is at $H \cong 232$ kOe, i.e., not far below 240 kOe. This means that the two MS's in Fig. 9 are the second and third members ($n=2,3$) of the second series. The first member ($n=1$) is expected to be near 80 kOe. It so happens that the second member of the first series is just below 80 kOe, so that the first member of the second series and the second member of the *first series* nearly coincide. As discussed later, the size δM of a step in the first series should be considerably larger than that for a step in the second series. For this reason the first step of the second series is masked by the second step of the first series.

In summary, there are two series of MS's. The first series consists of the first three MS's in Fig. 8(a) or Fig. 8(b). The first two MS's in Fig. 6(a) or Fig. 6(b) are the second and third members of this first series. As for the second series, its second and third members are the MS's in Fig. 9. The first member of the second series is obscured by the second member of the first series. The highest-field MS in Figs. 6, 7, and 8 is the second member of the second series.

The exchange constants J_i associated with the two series were obtained from the field separations $(H_{n+1}-H_n)$ using Eq. (8) with J_1 replaced by J_i. The value $g=2.297$ for Co^{2+} in ZnTe was used.[25] This procedure gave $J_i/k_B=-(2.7\pm0.3)$ K for the first series, and $-(5.7\pm0.6)$ K for the second. Both exchange constants must be associated with distant neighbors, because the NN exchange constant is $J_1/k_B=-38$ K (Ref. 5).

B. Identification of the two series

Several methods were used to identify the two series, i.e., assign each of them to a particular type of pairs asso-

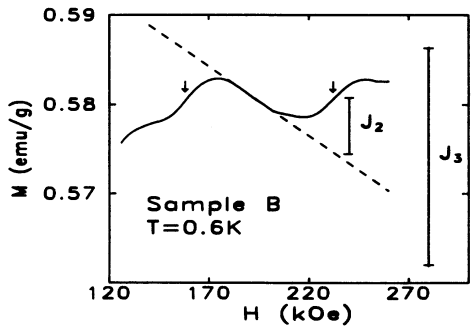

FIG. 9. The solid curve shows the upper portion of the magnetization curve of sample B at 0.6 K. These data were taken in the 27 T hybrid magnet. The two MS's in this field range are indicated by arrows. The bars show the calculated sizes for a J_2 step and for a J_3 step. The dashed line is an extrapolation of the data between the two MS's.

ciated with a particular distant-neighbor exchange constant J_i. All methods led to the conclusion that the second series (at the higher fields) is due to J_2 pairs, whereas the first series is due to J_3 pairs.

The expected sizes of the J_2 steps, J_3 steps, and J_4 steps were calculated. Here, use was made of the known value of x, the results in Fig. 4, and the known g factor.[25] The calculated size δM for each of these three series turned out to be much larger than the resolution of the present magnetization measurements. Thus, none of these series should have been missed because of inadequate experimental resolution. A second condition for observing a series is that it must occur within the available field range. The upper limit for the observable $|J_i|$ is then set by the maximum available magnetic field [the analog of Eq. (7), with $n=1$]. In the present experiments the largest observable $|J_i|/k_B$ was 21 K, which is above half the value of $|J_1|/k_B$. Because J_2/J_1 is expected to be well below 0.5, the J_2 steps should have been observed. Assuming that the J_i's decrease in magnitude with the distance r_i, it then follows that the largest J_i observed in the present work (for the second series) was J_2. The next largest observed J_i (for the first series) was then J_3.

Another method of identifying the series was based on a comparison between the observed and calculated size δM of each step. In both Fig. 6(a) and Fig. 9 the calculated sizes for a J_2 step and for a J_3 step are shown as bars. The size of a J_3 step is significantly larger. There were large uncertainties in the *observed* sizes because the MS's were small, and because they were superimposed on a monotonic variation of M. Nevertheless, the size of the steps in the second series [both MS's in Fig. 9, and the highest-field MS in Fig. 6(a)] seemed to agree better with J_2 steps than with J_3 steps. For the first series [e.g., the second MS in Fig. 6(a)] the size was consistent with J_3 steps.

The *relative* sizes of the MS's in the two series also seems to support the preceding assignments. The data in Figs. 8(a) and 8(b) suggest that the MS at the highest field, which belongs to the second series, is smaller than the other three MS's, or at least is not larger. For the present value of x, the J_2 steps should be much smaller than the J_3 steps. On the other hand, the J_3 steps are predicted to be significantly larger than the J_4 steps. Thus, the second and first series are consistent with J_2 and J_3 steps, respectively, but not with J_3 and J_4 steps, respectively. Some of the assignments for the various MS's are indicated in Figs. 6(b) and 8(b) as J_2, J_3, and $J_2 \& J_3$ (when they overlap).

C. Exchange constants and their ratios

Based on the above assignments, the second- and third-neighbor exchange constants are $J_2/k_B = -(5.7\pm0.6)$ K, and $J_3/k_B = -(2.7\pm0.3)$ K. These values should be compared with the dominant exchange constant $J_1/k_B = -38$ K, determined by Giebultowicz *et al.* using neutron diffraction.[5]

The ratio $J_2/J_1 = 0.15$ is comparable to the ratio 0.09 given by Eq. (1), which is the prediction of Larson *et al.* for Mn-based II-VI DMS's. The observed J_2/J_1 ratio also agrees with the suggested algebraic dependence $J(r) \propto r^{-n}$, if $n = 5.5$. Of greater significance, in our view, is the fact that the experimental result for J_2/J_1 supports the generally held belief that in II-VI DMS's, J_2 is an order of magnitude smaller than J_1.

The observed ratio $J_3/J_2 = 0.47$ is substantially higher than the value 0.09 given by Eq. (1). This equation, however, was obtained specifically for Mn^{2+} ions. Apparently it does not apply to Co^{2+} ions. The algebraic dependence $J \propto r^{-n}$, with n between 5 and 8, implies that J_3/J_2 is in the range 0.20 to 0.36. The experimental ratio 0.47 is outside this range. The deviation from the algebraic dependence is not too surprising, since this dependence was proposed on purely empirical grounds. The data on which the relation $J \propto r^{-n}$ is based involve the added contributions of several, or many, exchange constants.[9,10] These data seem to suggest that the algebraic dependence represents the general trend of J vs r, but they do not necessarily imply that this dependence is accurate for each individual J_i. There is also some doubt, based on theory, as to whether the algebraic dependence represents the correct general trend at large r (Ref. 3).

The measured ratio $J_3/J_2 \cong 1/2$ is in excellent agreement with the suggestion of Bruno and Lascaray, Eq. (2). At present it is not known whether their suggestion will also hold for other II-VI DMS's. Some preliminary results which were obtained earlier[13] for $Zn_{1-x}Co_xSe$ ($J_3/J_2 \cong 1/4$) suggest that it will not.

ACKNOWLEDGMENTS

The work at Tufts University was supported by National Science Foundation (NSF) Grant No. DMR-8900419. The equipment for the magnetometry facility at Tufts was donated by the W. M. Keck Foundation. The work at Brown University was supported by NSF grant No. DMR-8901270. The Francis Bitter National Magnet Laboratory is supported by NSF. V.B. was supported by the University of São Paulo, and C.C.A. was supported by IBM.

*On leave from the University of São Paulo, São Paulo, Brazil.

[1]B. E. Larson, K. C. Hass, H. Ehrenreich, and A. E. Carlsson, Phys. Rev. B **37**, 4137 (1988); **38**, 7842E (1988).

[2]B. E. Larson and H. Ehrenreich, J. Appl. Phys. **67**, 5084 (1990).

[3]K. C. Hass, in *Semimagnetic Semiconductors and Diluted Magnetic Semiconductors,* edited by M. Averous and M. Balkanski (Plenum, New York, 1991), p. 59.

[4]J. Spalek, A. Lewicki, Z. Tarnawski, J. K. Furdyna, R. R. Galazka, and Z. Obuszko, Phys. Rev. B **33**, 3407 (1986); A. Lewicki, A. I. Schindler, J. K. Furdyna, and W. Giriat, Phys. Rev. B **40**, 2379 (1989).

[5]T. M. Giebultowicz, J. J. Rhyne, J. K. Furdyna, and P. Klosowski, J. Appl. Phys. **67**, 5096 (1990); L. M. Corliss, J. M. Hastings, S. M. Shapiro, Y. Shapira, and P. Becla, Phys. Rev. B **33**, 608 (1986).

[6]Y. Shapira, J. Appl. Phys. **67**, 5090 (1990).

[7]Y. Shapira, in *Semimagnetic Semiconductors and Diluted Magnetic Semiconductors,* edited by M. Averous and M. Balkanski (Plenum, New York, 1991), p. 121.

[8]W. J. M. de Jonge and H. J. M. Swagten, J. Magn. Magn. Mater. **100**, 322 (1991).

[9]A. Twardowski, H. J. M. Swagten, W. J. M. de Jonge, and M. Demianiuk, Phys. Rev. B **36**, 7013 (1987).

[10]A. Lewicki, A. I. Schindler, I. Miotkowski, B. C. Crooker, and J. K. Furdyna, Phys. Rev. B **43**, 5713 (1991); H. J. M. Swagten, A. Twardowski, E. W. Janse, P. J. T. Eggenkamp, and W. J. M. de Jonge, J. Magn. Magn. Mater. **104-107**, 989 (1992).

[11]A. Bruno and J. P. Lascaray, Phys. Rev. B **38**, 9168 (1988).

[12]B. E. Larson, K. C. Hass, and R. L. Aggarwal, Phys. Rev. B **33**, 1789 (1986).

[13]Y. Shapira, T. Q. Vu, B. K. Lau, S. Foner, E. J. McNiff, Jr., D. Heiman, C. L. H. Thieme, C.-M. Niu, R. Kershaw, K. Dwight, A. Wold, and V. Bindilatti, Solid State Commun. **75**, 201 (1990).

[14]H. A. Weakliem, J. Chem. Phys. **36**, 2117 (1962).

[15]M. Villeret, S. Rodriguez, and E. Kartheuser, Phys. Rev. B **41**, 10 028 (1990); Physica B **162**, 89 (1990).

[16]Y. Shapira, S. Foner, D. H. Ridgley, K. Dwight, and A. Wold, Phys. Rev. B **30**, 4021 (1984).

[17]R. E. Behringer, J. Chem. Phys. **29**, 537 (1958).

[18]M. M. Kreitman and D. L. Barnett, J. Chem. Phys. **43**, 364 (1965).

[19]O. Okada, J. Phys. Soc. Jpn. **48**, 391 (1980).

[20]V. Bindilatti, T. Q. Vu, Y. Shapira, C. C. Agosta, E. J. McNiff, Jr., R. Kershaw, K. Dwight, and A. Wold, Phys. Rev. B **45**, 5328 (1992).

[21]U. W. Pohl and W. Busse, J. Chem. Phys. **90**, 6877 (1989). Some of the results for triplets in this reference differ from those in the earlier work by Okada (Ref. 19).

[22]When J_3/J_2 is as large as 0.5, the fine structure in the J_2 steps is more complicated. Consider a J_2 step corresponding to a particular value of n. Because J_3 is not small, J_2 steps which involve a J_3 bond attached to the J_2 pair (e.g., the J_2+ MS due to the J_2-J_3 open triplets) are well separated from other special types of J_2 steps, which do not involve such a J_3 bond (e.g., the MS's arising from pure J_2 pairs, or from J_2-J_4 open triplets). The MS's with no J_3 bond may not be resolved from each other even though they are resolved from the MS's that involve a J_3 bond. When this is the case, the unresolved MS's (with no J_3 bond) form a single J_2 step. Such a J_2 step, with no fine structure, exists for each value of n. When the various values of n are considered, one obtains a series of J_2 steps ($n=1,2,3$) with no resolved fine structure in each step. Equation (8), with J_1 replaced by J_2, applies to this series. The size of the steps in this series is governed by the number of pure J_2 pairs in the J_1-J_2-J_3 model (not in the J_1-J_2 model). In addition to this series there are also the J_2 steps that involve a J_3 bond. For the concentration x in the present samples, the J_2 steps that involve a J_3 bond are difficult to observe because of their small size.

[23]A. G. Swanson, Y. P. Ma, J. S. Brooks, R. M. Markiewicz, and N. Miura, Rev. Sci. Instrum. **61**, 848 (1990).

[24]Y. Shapira, S. Foner, P. Becla, D. N. Domingues, M. J. Naughton, and J. S. Brooks, Phys. Rev. B **33**, 356 (1986).

[25]F. S. Ham, G. W. Ludwig, G. D. Watkins, and H. H. Woodbury, Phys. Rev. Lett. **5**, 468 (1960).